

Assessing Climate Change Impacts in the Tana Basin, Ethiopia

BAGTZOGLU A.^{1,*}, KHADIM F.¹, DOKOU Z.², LAZIN R.¹, ANAGNOSTOU E.¹,

¹Department of Civil and Environmental Engineering, 261 Glenbrook Road, University of Connecticut, Storrs, CT 06269, USA

²Department of Civil Engineering, California State University, Sacramento, CA 95819, USA

*corresponding author:

e-mail: amvrossios.bagtzoglou@uconn.edu

Abstract Climate change effects on long-term groundwater (GW) resource developments in the Tana Basin, Ethiopia, were investigated using a fine-resolution GW model based on MODFLOW-NWT. The GW model was calibrated with 98 historical instantaneous well-level measurements and 38 years of monthly lake level data. Using this model we simulated long-term climate change impacts by considering two representative concentration pathways (RCPs) from the two extreme global circulation models available in the region. While the MIROC5 simulated GW table (GWT) was found to be stable, the CSIRO-Mk3 simulated GWT exhibited large fluctuations (+2 m to -4 m) by 2100 due to climate change. More critical impacts were predicted for the lake, where total lake releases from the baseline scenario were projected to change by +50% (MIROC5) or -22% (CSIRO-Mk3) by the end of 2100.

Keywords: groundwater model; sustainability; MODFLOW-NWT; Upper Blue Nile

1. Introduction

Almost 50% of the population in Africa that relies on GW is projected as being exposed to climate vulnerability (Haile et al., 2020; Tenagashaw and Andualem, 2022). In Ethiopia, climate change in combination with growing water/food and anthropogenic stresses may impose a substantial risk to its rich reserves of GW resources, straining the country's development needs. The country's climate vulnerability is critical due to its rainfed irrigation dependency, severe agricultural drought, unsustainable use of resources, and existing water/food security issues (Gebrehiwot and van der Veen, 2013; Lewis, 2017)). Climate variability could affect the GW system's direct replenishment through recharge and future GW use patterns needed to sustain the country's needs in the domestic, industrial, and agricultural sectors. In order to address these concerns we simulated the long-term impacts of climate change on the GW resources of the Tana Basin and the SW-GW budget in Lake Tana itself, using a calibrated GW model.

The simulations in this paper take the recharge, streamflow, and lake evaporation outputs from the Coupled Routing and Excess STorage (CREST)

hydrological model simulations performed in our group (Lazin et al., 2020) and develop a fine-resolution (500 m) calibrated GW model for a spatial domain encompassing the Tana Basin. Overland precipitation and evaporation, which come from satellite, reanalysis, and CREST simulations, respectively, are inputs to the model. The model was calibrated with 98 instantaneous observation wells from 2013–2017, located across the Tana Basin and was used to perform long-term simulations up to 2100. We used two climate change scenarios for the two general circulation models (GCMs), e.g., RCP 4.5 and RCP 8.5 to pass the meteorological forcings to CREST. We then simulated recharge, streamflow, and lake evaporation using CREST, which were added as inputs to the Tana Basin GW model.

2. Study Area

The model domain covers the Tana Basin which has an area of 15,096 km². The topographic relief varies from an elevation of 4509 m on the east to an elevation of 1777 m near Lake Tana. Lake Tana is the largest lake in Ethiopia, accounting for 50% of the freshwater resources for the country, including water for domestic use, irrigation, hydropower production, fisheries, grazing, and livestock. Lake Tana is an important source of fish for communities around the lake and beyond, while the lake wetlands are very important for breeding and enhancing biodiversity, sediment retention, and flood protection.

3. Groundwater Modeling

In this work, we modified our previous model (Khadim et al., 2020) by extending it to encompass the entire Tana Basin and simulating the water levels and lake-aquifer interactions in Lake Tana, using MODFLOW's Lake Package. The stratigraphy is based on the work of Hautot et al. (2006). The numerical model included two aquifers; the bottom aquifer was always confined, and the top aquifer was unconfined. The spatially varying thickness of the top layer was obtained by kriging interpolation based on borehole depth records of the 98 observation wells. The GW model was calibrated to minimize the root mean squared error between simulated and observed heads, from the 98 historical wells.

We used the climate projections from a Regional Climate Model (RCM), named Rossby Centre Atmospheric Model version 4 (RCA4) for representative concentration pathways (RCP) 4.5 and 8.5 (IPCC, 2013). The RCA4 model provides an ensemble of future climate change scenarios (Kjellstrom et al., 2016). In this RCM, relevant hydrometeorological parameters are downscaled to a resolution of 3 hours and 50 km from different GCMs of the Coupled Model Intercomparison Project 5 (Taylor et al., 2012). In order to analyze the impact of future extremes, we selected the wettest (MIROC5) and driest (CSIRO-Mk3) GCMs from all available downscaled GCM products in the RCA4 model.

4. Climate Change Impacts

We investigated a range of potential impacts of climate change on the physical availability of GW resources in the Tana Aquifer. The analyses were conducted in four different time periods: a baseline period 1991–2020, an early-century period 2021–2050, a mid-century period 2051–2080, and a late-century period 2081–2100. We investigated time-series estimates of lake levels, spatiotemporal estimates of GW head (H), GW depletions and future lake and reservoir management at regional and local scales.

We used the standardized water level index (SWI) defined by Bhuiyan (2004) to infer GW depletions by estimating the normalized differences (with respect to standard deviation) of GW levels from the baseline mean (where positive values indicate a drop in water levels). The method has found wide acceptance due to its generalizability in different parts of the world (Roshun and Roshan, 2018), and more specifically, in Ethiopia (Edossa et al., 2008). SWI values within 0–1 are classified as mild depletion, while values from 1–2.5 refer to moderate, 2.5–4 refer to severe, and >4 refer to extreme GW depletions.

5. Results and Discussion

5.1 Groundwater Table

The climate change impacts on the GWT in the model domain are shown in Figure 1. The average depth of GWT for the baseline period is shown in Figure 1a. The figure shows relatively shallow (within a depth of 5 m from the surface, marked by a blue color) groundwater availability along the major river routes in the Tana Basin. There are some regions where the GWT drops to moderate depths of up to 30 m. In some areas with high elevations in the south and east, the areas within the northern flood plains, and the Megech sub-basin regions, the GWT dropped approximately 40–50 m. The figure also shows a contour map of simulated hydraulic heads, H, for the baseline simulation period (Figure 1d).

Figure 1b1, c1 shows the comparison between the long-term simulated GW levels when are forced with the two RCP projections (4.5 and 8.5) of the wettest (MIROC5) and driest (CSIRO-Mk3) climate models. The figures represent the temporally averaged anomalies of GW levels for three different 30-year spans up to 2100 (2020–2050,

2051–2080, and 2081–2100), in comparison with the baseline GW levels shown in Figure 1a. Water gains and losses are represented by blue and red shades in Figure 1b1, c1, respectively. Figure 1b2, c2 also provide boxplots showing the spread of individual data points. The boxplots presented in Figure 1 showcase the 5% and 95% quantiles (transect lines) and the 25% and 75% quantiles (solid rectangles).

From the baseline scenario, the MIROC5 RCP 4.5 simulated mean GWT changed by +0.05 m, +0.1 m, and +0.02 m during the 2021–2050, 2051–2080, and 2081–2100 periods, respectively. The MIROC5 RCP 8.5 simulated mean GWT changed by +0.11 m, +0.09 m, and +0.1 m during the 2021–2050, 2051–2080, and 2081–2100 periods, respectively. The CSIRO-Mk3 RCP 4.5 simulated mean GWT changed by +0.01 m, –0.35 m and –0.6 m during the 2021–2050, 2051–2080, and 2081–2100 periods, respectively. Finally, the MIROC5 RCP 8.5 simulated mean GWT changed by –0.01 m, –0.4 m, and –0.8 m during the 2021–2050, 2051–2080, and 2081–2100 periods, respectively.

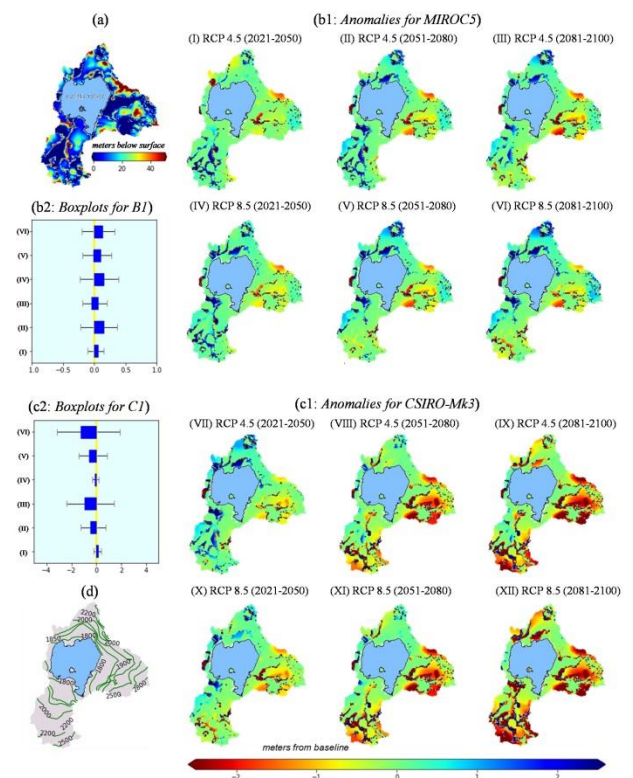


Figure 1. Climate change impacts on Tana GWT (a): average depth of GWT for the period 1991–2020, (b1): deviations of GWT from baseline for MIROC5 model, (b2): boxplots of individual data points used in (b1); (c1): deviations of GWT from baseline for CSIRO-Mk3 model, (c2): boxplots of individual data points used in (c1); (d): average hydraulic head.

The monthly GW level simulations for future climate events, did not indicate any ‘moderate’ or worse GW depletions (e.g., SWI > 1) when compared with the baseline scenario (1991–2020). Figure 2 shows the number of months in a year when each model grid was predicted to be subjected to ‘mild’ depletion. Areas of mild depletion exhibited in MIROC5 RCP 4.5 simulations were 20%, 18%, and 22% during the 2021–2050, 2051–2080, and 2081–2100 periods, respectively. MIROC5 RCP 8.5

simulated estimates were 17%, 18%, and 16% during the 2021–2050, 2051–2080, and 2081–2100 periods, respectively. In contrast, areas of mild depletions for CSIRO-Mk3 RCP 4.5 simulations were 17%, 32%, and 48% during the 2021–2050, 2051–2080, and 2081–2100 periods, respectively. Finally, CSIRO-Mk3 RCP 8.5 simulated estimates were 21%, 46%, and 68% during the 2021–2050, 2051–2080, and 2081–2100 periods, respectively.

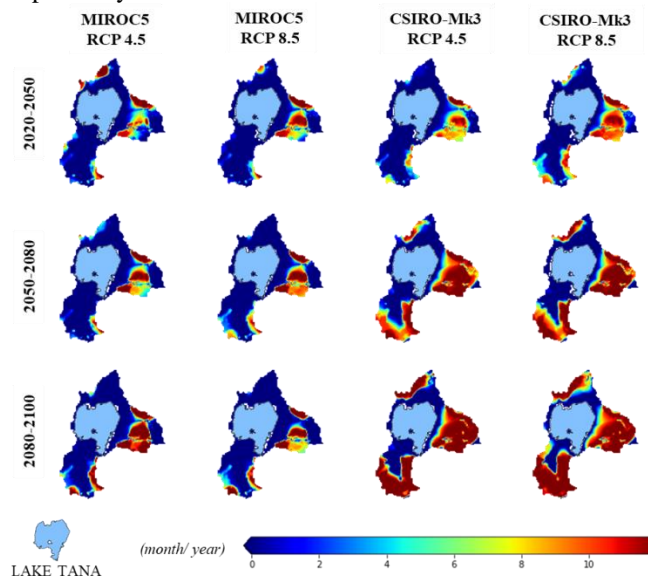


Figure 2. Number of months per year with mild GW depletions ($1 > SWI > 0$) for the Tana Basin.

5.2 Lake Tana Dynamics

The lake inflows (accounting for both SW and GW contributions) were estimated as 1675 mm/yr. Outflows (through the Blue Nile outlet releases, GW outflow, plus withdrawals) for the baseline scenario (1991–2020) were estimated as 1666 mm/yr. In order to investigate the climate change effects on future water levels and releases of Lake Tana, we simulated our calibrated GW model up to 2100 under the four different projections (e.g., RCP 4.5 and RCP 8.5 for the two climate models). For future climate simulations, we used MODFLOW's LAK package to simulate river releases through the outlet in a way so that the lake levels vary within a specified threshold (1784 m to 1787 m, per regulatory standard), and all water budget components are balanced, accounting for the withdrawal, for hydropower and domestic purposes. These results are not included here due to space constraints.

5.3 Future Impacts and Water Management

In Figure 1 the averaged GW level anomalies varied from +2 m to –4 m from baseline estimates. More water gain was exhibited for the wet climate model, MIROC5, whereas the dry climate model, CSIRO-Mk3, led to significant water losses. Water losses for the dry climate model were more prominent in high-elevation areas, e.g., east of the Ribb and Gumera sub-basins, and south of the Gilgel-Abay sub-basin. Among the two different projections, RCP 8.5 indicated more extreme water loss (for the CSIRO-Mk3 model). MIROC5 RCP 8.5 forced GW levels were found higher than MIROC5 RCP 4.5.

5.4 Study Limitations

This study experienced several limitations, most notably, the scarcity of continuous records of GW levels in the Tana Basin. Another limitation of the study is the internal validity attributed to using future scenarios without considering detailed anthropogenic or land use processes. Finally, from a simulation standpoint, a limitation was not being able to consider an ensemble of GCMs to force our models, which was not possible due to computational expense.

6. Conclusions

We used a physically-based numerical model to improve on our previous efforts and then used the newly calibrated Tana GW model to simulate long-term climate change projections by considering two extreme GCMs (MIROC5 and CSIRO-Mk3) by assessing RCPs 4.5 and 8.5. The simulated hydraulic head values indicate a substantial physical availability of GW resources in the future, especially in areas closer to Lake Tana. The long-term climatic simulations carried out in this study provide an important source of information for regional policy and decision-makers, which may be used as a basis for other cross-cutting research.

Acknowledgements This research is based upon work supported by the National Science Foundation under Grant No. 1545874.

References

- Bhuiyan, C. Various drought indices for monitoring drought condition in Aravalli terrain of India. In Proc. of the XXth ISPRS Congress, Istanbul, Türkiye, **2004**; p. 12–23.
- Edossa, D.C.; Babel, M.S.; Gupta, A.D. Drought analysis in the Awash river basin, Ethiopia. *Water Resour. Manag.* **2010**, *24*, 1441–1460.
- Gebrehiwot, T.; van der Veen, A. Assessing the evidence of climate variability in the northern part of Ethiopia. *J. Dev. Agric. Econ.* **2013**, *5*, 104–119.
- Haile, G.G.; Tang, Q.; Hosseini-Moghari, S.; Liu, X.; Gebremicael, T.G.; Leng, G.; Kebede, A.; Xu, X.; Yun, X. Projected Impacts of Climate Change on Drought Patterns Over East Africa. *Earth's Future* **2020**, *8*, e2020EF001502.
- Hautot, S.; Whaler, K.; Gebru, W.; Desissa, M. The structure of a Mesozoic basin beneath the Lake Tana area, Ethiopia, revealed by magnetotelluric imaging. *J. Afr. Earth Sci.* **2006**, *44*, 331–338.
- IPCC. *Summary for Policymakers in Climate Change 2013: The Physical Science Basis*; Contribution of Working Group I to the Fifth Assessment Report of the Intergovernmental Panel on Climate Change; Stocker, T.F., et al. Eds.; Cambridge University Press: Cambridge, UK; New York, NY, USA, **2013**.
- Khadim, F.K.; Dokou, Z.; Lazin, R.; Moges, S.; Bagtzoglou, A.C.; Anagnostou, E. Groundwater Modeling in Data Scarce Aquifers: The case of Gilgel-Abay, Upper Blue Nile, Ethiopia. *J. Hydrol.* **2020**, *590*, 125214.

- Kjellström, E.; Barring, L.; Nikulin, G.; Nilsson, C.; Persson, G.; Strandberg, G. Production and use of regional climate model projections—A Swedish perspective on building climate services. *Clim. Serv.* **2016**, *2*, 15–29.
- Lazin, R.; Shen, X.; Koukoulou, M.; Anagnostou, E. Evaluation of the Hyper-resolution Model Derived Water Budget Components over the Upper Blue Nile Basin. *J. Hydrol.* **2020**, *590*, 125231.
- Lewis, K. Understanding climate as a driver of food insecurity in Ethiopia. *Clim. Chang.* **2017**, *144*, 317–328.
- Roshun, S.H.; Roshan, M.H. Monitoring of Temporal and Spatial Variation of Groundwater Drought using GRI and SWI Indices (Case Study: Sari-Neka Plain). *J. Watershed Manag. Res.* **2018**, *9*, 269–279.
- Taylor, K.E.; Stouffer, R.J.; Meehl, G.A. An Overview of CMIP5 and the Experiment Design. *Bull. Am. Meteorol. Soc.* **2012**, *93*, 485–498.
- Tenagashaw, D.Y.; Andualem, T.G. Analysis and Characterization of Hydrological Drought Under Future Climate Change Using SWAT Model in Tana Sub-basin, Ethiopia. *Water Conserv. Sci. Eng.* **2022**, *7*, 131–142.